

DATING THE FORMATION OF JUPITER USING THE DISTINCT GENETICS AND FORMATION TIMES OF METEORITES

T.S. Kruijer^{1,2}, C. Burkhardt¹, G. Budde¹, T. Kleine¹. ¹Institut für Planetologie, University of Münster, Münster, Germany. ²Lawrence Livermore National Laboratory, Livermore, CA, USA. (*kruijer1@llnl.gov)

Introduction: Gas-giant planets, including Jupiter, likely formed through the growth of large solid cores, followed by the accumulation of gas onto these cores [e.g. 1]. Dating the formation of Jupiter is key for understanding the early evolution of the solar system and planetary accretion [e.g. 2]. However, until now it has not been possible to date Jupiter's growth. Prior work revealed a fundamental genetic dichotomy distinguishing between carbonaceous (CC) and non-carbonaceous (NC) meteorite reservoirs [3]. This dichotomy either reflects a temporal change in disk composition or the spatial separation of materials accreted inside (NC) and outside (CC) the orbit of Jupiter [2-4]. If the latter is correct, then the formation of Jupiter can be dated by assessing the formation time and lifetime of the NC and CC reservoirs. However, it is currently unclear when these reservoirs formed, and if and for how long they remained isolated. To address this, we obtained Mo and W isotopic data for iron meteorites. These derive from some of the earliest planetesimals, making them ideal samples to search for the effects of Jupiter's growth on solar nebula dynamics. For this study we analysed a large set of iron meteorites, determined the time of core formation on their parent bodies using ¹⁸²Hf-¹⁸²W chronometry and used Mo isotopes to link the irons to the NC or CC meteorites.

Results: In a plot of $\epsilon^{95}\text{Mo}$ vs. $\epsilon^{94}\text{Mo}$ (parts per 10⁴ deviations from terrestrial standard values), the iron meteorites analysed here and in prior work [5] define two distinct s-process mixing lines (Fig. 1). Thus, similar to chondrites [3,4], iron meteorites derive from two genetically distinct NC and CC nebular reservoirs. A similar genetic dichotomy is seen for W isotopes, where the NC irons have lower $\epsilon^{182}\text{W}$ and no nucleosynthetic anomalies (i.e., $\epsilon^{183}\text{W} \sim 0$), whereas the CC irons have higher $\epsilon^{182}\text{W}$ and nucleosynthetic $\epsilon^{183}\text{W}$ excesses (Fig. 2).

Discussion: The higher $\epsilon^{182}\text{W}$ of CC irons most likely reflects a later time of core formation compared to NC irons (Fig. 2), which in turn likely reflects different accretion times of <0.4 Ma (NC irons) and ~1 Ma (CC irons). Moreover, given that parent body accretion in both reservoirs occurred within <1 Ma after CAIs, the NC and CC reservoirs must already have been separated by this time. The timespan over which these reservoirs remained separated can be inferred from chondrites, whose parent bodies accreted at ~2 Ma in the NC reservoir (ordinary chondrites) and until at least ~4 Ma in the CC reservoir (carbonaceous chondrites) [e.g. 6]. As no meteorites plot between the CC- and NC-lines (Fig. 1), the NC and CC reservoirs remained isolated from each other until parent body accretion ended at >4 Ma after CAIs.

The only plausible mechanism that can efficiently separate the NC and CC reservoirs for this extended period of time is the formation of Jupiter [e.g. 2,7]. The growth of Jupiter beyond >20 Earth masses (M_E) inhibited the inward drift of small particles [7], implying that at the time the CC reservoir formed (i.e., ~1 Ma after CAI), Jupiter already had a size of >20 M_E . Once Jupiter reached a mass of 50 M_E , a gap opened in the disk, which was followed by scattering of bodies from beyond Jupiter's orbit (i.e., CC bodies) into the inner solar system [8]. This scattering of CC bodies cannot have started before ~4 Ma, because CC bodies continued to form until at least that time. Thus, Jupiter must have reached ~50 M_E later than ~4 Ma after CAIs.

References: [1] Pollack J.B. et al. (1996) *Icarus* **124**, 62–85. [2] Morbidelli A. et al. (2016) *Icarus* **267**, 368–376. [3] Warren P.H. (2011) *EPSL* **311**, 93–100. [4] Budde G. et al. (2016) *EPSL* **454**, 293–303. [5] Burkhardt C. et al. (2011) *EPSL* **312**, 390–400. [6] Kita N.T. & Ushikubo T. (2012) *MAPS* **47**, 1108–1119. [8] Walsh K.J. et al. (2011) *Nature* **475**, 206–209. Work was performed under the auspices of the U.S. DOE by LLNL under Contract DE-AC52-07NA27344.

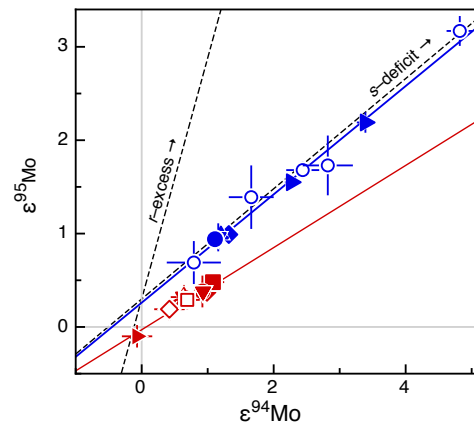


Fig. 1: Iron meteorites (closed symbols) and chondrites (open symbols) show two distinct trends, separating a carbonaceous (blue) from a non-carbonaceous reservoir (red).

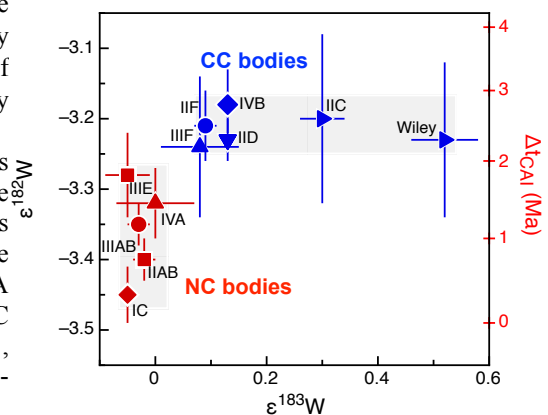


Fig. 2: Tungsten isotope dichotomy of iron meteorites.